Journal of Materials Chemistry A

PAPER

View Article Online
View Journal | View Issue

Cite this: J. Mater. Chem. A, 2016, 4, 13265

An effective way to reduce energy loss and enhance open-circuit voltage in polymer solar cells based on a diketopyrrolopyrrole polymer containing three regular alternating units†

Yahui Liu,[a] Guangwu Li,[a] Zhe Zhang,[a] Liangliang Wu,[a] Jianya Chen,[b] Xinjun Xu,*[a] Xuebo Chen,[a] Wei Ma[b] and Zhishan Bo*[a]

Received 29th June 2016
Accepted 28th July 2016

DOI: 10.1039/c6ta05471d

www.rsc.org/MaterialsA

A novel diketopyrrolopyrrole (DPP)-based conjugated polymer (**PCDPP**) was designed, synthesized and used as a donor material for polymer solar cells (PSCs). By increasing the planarity of polymer chains and reducing the energy loss in devices, we have simultaneously acquired a high short-circuit current (J_{sc}) and a large open-circuit voltage (V_{oc}) in PSCs based on **PCDPP**, which is a regular alternating ternary conjugated polymer. This polymer has a medium optical band gap (1.55 eV) with low-lying HOMO and LUMO energy levels. In addition, **PCDPP** exhibits a very good planarity from density functional theory (DFT) calculations and forms a fibrillar network in the active layer of solar cells. Because of these integrated favourable effects, **PCDPP**-based photovoltaic devices exhibit a high power conversion efficiency (PCE) of 9.02% which is among the highest values reported so far for devices based on DPP-containing polymers. More importantly, the V_{oc} of our **PCDPP**-based devices can reach as high as 0.86 V, which is much higher than that (<0.7 V) of high-efficiency solar cells based on other DPP polymers. These results provide a promising way to minimize the energy loss and to realize high V_{oc} and J_{sc} values at the same time in devices to obtain high power conversion efficiencies.

Introduction

Conjugated polymers employing diketopyrrolopyrrole, namely, 2,5-dihydropyrrolo[4,3-*c*]pyrrolo-1,4-dione (DPP) units, are widely used as donor materials in bulk heterojunction (BHJ) polymer solar cells.[1–6] When mixed with fullerene derivatives such as [6,6]-phenyl-C_{71}-butyric acid methyl ester ($PC_{71}BM$), DPP-based polymers can form efficient interpenetrating networks in blend films, which is beneficial to exciton diffusion and charge transport. Besides, the DPP moiety has a polar nature that can promote the polymers to crystallize, so DPP-based polymers usually exhibit excellent charge carrier mobility, and high short-circuit current density (J_{sc}) and fill factor (FF). Also, their good charge transport abilities enable the realization of high-efficiency solar cells with a thick active layer, which is highly desirable for the inkjet-printed or screen-printed process with pinhole-free large areas at high printing rates.[7–9] However, most of the DPP-based polymers have a narrow bandgap (E_g) and exhibit a low open-circuit voltage (V_{oc}) in photovoltaic devices.[1,10,11] Due to their small V_{oc} values (usually less than 0.7 V), only a very few examples with power conversion efficiency (PCE) larger than 8% have been demonstrated in polymer solar cells containing a DPP-based polymer as the active layer.[1,9] To surmount this limitation, efforts have been made to increase the V_{oc} by lowering the HOMO energy level of polymers *via* adjusting the donor units in polymer main chains. As a result, a high V_{oc} larger than 0.8 V has been demonstrated.[12–18] Unfortunately, a relatively large photon energy loss (E_{loss}) (~0.8–1.0 eV), which is defined by $E_g - eV_{oc}$, where E_g is the optical bandgap of the semiconducting polymer evaluated from the absorption edge, usually exists in these systems. Thus, it is hard to realize a high J_{sc} and a high V_{oc} simultaneously, because it is a well-known fact that there is a trade-off between these two parameters. The reason lies in the fact that the realization of both high J_{sc} and V_{oc} requires that the polymer must have both a narrow E_g and a deep HOMO energy level. However, this will inevitably diminish the energy offset of the LUMOs between the polymer and fullerene, thus weakening the driving force for photo-induced charge separation. A key for minimizing this trade-off is to reduce the E_{loss} by synthesizing new conjugated polymers to manage the energetics between polymers and fullerenes.[19]

[a]Beijing Key Laboratory of Energy Conversion and Storage Materials, College of Chemistry, Beijing Normal University, Beijing 100875, China. E-mail: xuxj@bnu.edu.cn; zsbo@bnu.edu.cn; Tel: +86-10-62206891

[b]State Key Laboratory for Mechanical Behavior of Materials, Xi'an Jiaotong University, Xi'an 710049, China 710049. E-mail: msewma@mail.xjtu.edu.cn

† Electronic supplementary information (ESI) available. See DOI: 10.1039/c6ta05471d

As we know, the widely used multi-component copolymerization can adjust the optical band gap and orbital levels at the same time, and then energy loss and V_{oc} tuning can be achieved.[20,21] According to previous reports for random copolymers, 1D/2A (one donor unit and two acceptor units) or 2D/1A (two donor units and one acceptor unit) structures have been usually constructed.[21–25] However, the dissimilar chemical structure of comonomers, the random sequence in copolymer chains and the irregular chemical structure may cause infaust effects on molecular packing, charge transport, and the macroscopic properties of polymers.[26–28] In contrast, besides adjusting the optical band gaps and orbital levels in polymers, regular alternating ternary copolymerization allows the synthesis of regioregular polymers, which have a regular and alternating structure oriented along the chain.[29,30] Such regioselectivity in polymerizations is of great help to suppress variations in the molecular order and facilitate intermolecular π-stacking interactions which in turn can increase charge transport through polymer films.

It is quite important to select suitable regular alternating units for performance improvement. As we all know, the introduction of fluoro atoms can lower the energy level of polymers, so 3,6-difluorocarbazole was used as one of the donor units. And then, the insertion of 3,6-difluorobenzene can modify the chemical geometry, which is expected to enhance the planarity of the polymer backbone. In this communication, regular alternating ternary copolymerization was carried out to get **PCDPP** comprising two donor segments (2,5-difluorobenzene and difluorocarbazole) and one acceptor unit (DPP). This polymer has a medium optical band gap (1.55 eV) and appropriate energy levels, which endow the corresponding solar cells with a high V_{oc} (0.86 V) and a small energy loss (0.69 eV). From density functional theory (DFT) calculations, we get that **PCDPP** displays a very planar chemical structure, which guarantees its good hole-transport ability, and thus higher J_{sc}. Combining these advantages, **PCDPP** exhibits an excellent photovoltaic performance, providing a high PCE of 9.02% which is among the highest values reported so far for solar cells using DPP-based polymers.[9,11] We should note that the V_{oc} of our device is much higher than that of other DPP-based polymers (<0.7 V) with high device efficiency. Given that in single-junction polymer solar cells V_{oc} can hardly be increased but J_{sc} can be increased by developing suitable charge collecting layers, we think our DPP-based polymer will be a promising candidate for potential applications in high-performance solar cells.

Results and discussion

The synthetic route of **PCDPP** is shown in Fig. 1. The starting materials **1**, **2** and **5** were synthesized according to the previous literature.[2,31,32] Compound **3** was synthesized through Suzuki coupling with a Pd catalyst. Monomer **4** was prepared from **3** by bromination with *N*-bromosuccinimide (NBS). Then, **PCDPP** was synthesized by Suzuki polymerization of monomers **4** and **5**. The polymer was first Soxhlet extracted with methanol, acetone, hexane, dichloromethane and chloroform, and then the residue was dissolved in boiling 1,1,2,2-tetrachloroethane

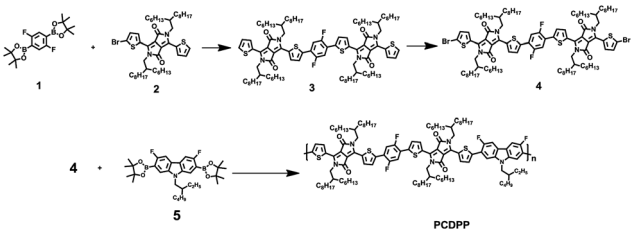

Fig. 1 Synthetic route of PCDPP.

(TCE) and precipitated into methanol, and the resultant solid was collected by filtration and dried under high vacuum. The detailed synthetic procedures are shown in the ESI.† The molecular weight of **PCDPP** was determined by gel permeation chromatography (GPC) at 80 °C using chlorobenzene as an eluent calibrated with polystyrene standards which afforded a high molecular weight of M_n = 136 kg mol^{-1} and a polydispersity index (PDI) of 5.19. The thermal stability of **PCDPP** was investigated by thermogravimetric analysis (TGA) which exhibited an excellent thermal stability with a decomposition temperature (5% weight loss) of 402 °C. Differential scanning calorimetry (DSC) measurements showed no obvious glass transition for **PCDPP** in the range of 50 °C to 250 °C.

UV-vis absorption spectra of **PCDPP** in dilute chloroform solution and as a thin film are shown in Fig. 2a. In dilute CB solution, **PCDPP** showed three absorption peaks between 350 nm and 900 nm. The peak at the short wavelength (395 nm) can be attributed to the localized π–π* transition and the strong peaks in the long wavelength region (600–800 nm) can be ascribed to the delocalized π–π* transition caused by the internal charge transfer (ICT) interaction. The absorption spectrum was slightly blue-shifted by several nanometers after heating the CB solution to 100 °C and the shoulder peaks in the long wavelength region debased, reflecting the weakening of the aggregation of polymers. **PCDPP** exhibits broader absorption in the solid state than in dilute solution, which is consistent with the reported references.[33] The optical bandgap is calculated to be 1.55 eV according to the equation: $E_{g,opt} = 1240/\lambda_{onset}$. The electrochemical properties were investigated by cyclic voltammetry (CV). The highest occupied molecular orbital (HOMO) and the lowest unoccupied molecular orbital (LUMO) calculated from the onset oxidation and reduction potentials are −5.44

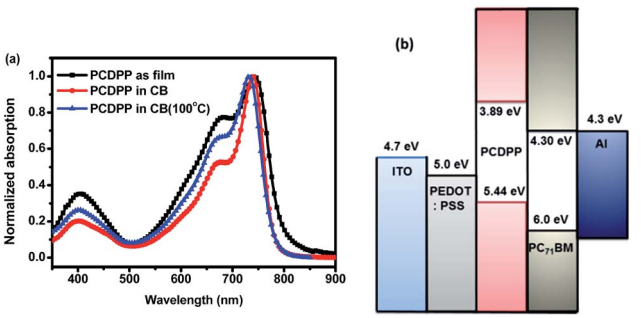

Fig. 2 UV-vis absorption spectra of PCDPP in CB and as a thin film (a) and the energy-band diagram (b).

and −3.89 eV, respectively. As we expected, the HOMO and LUMO levels of **PCDPP** significantly move down, which is beneficial to achieve higher V_{oc} and lower energy loss (0.69 eV). On the other hand, the LUMO level of **PCDPP** is 0.41 eV (>0.3 eV) higher than that of $PC_{71}BM$, which guarantees the formation of a downhill driving force for efficient exciton dissociation.[34,35] To directly observe the change of energy levels, the energy-band diagram is shown in Fig. 2b.

Density functional theory (DFT) calculations at the B3LYP/6-31G(d) level were also used to investigate the chemical geometries and electronic structures of the simplified repeating units and the alkyl side chain (see ESI†). As shown in Fig. 3, the dihedral angle between thiophene and 2,5-difluorobenzene, 3,6-difluorocarbazole is close to zero degrees in **PCDPP**, which is 0.04° and 0.02°, respectively. It is clear from the side view that **PCDPP** has a planar backbone. Compared with the D/A binary structure, in the 2D/1A ternary structure the introduction of 2,5-difluorocarbazole has two potential advantages: first, the backbone on **PCDPP** becomes a linear conformation; second, the density of the alkyl side chain which is disadvantageous for intermolecular π–π stacking is reduced with the insertion of 2,5-difluorobenzene. Hence, based on the DFT calculations, it can be predicted that this planar conformation may give rise to strong intermolecular interactions (π–π stacking) and a good charge transport ability and thus a high short circuit current. Moreover, this close π–π stacking (as mentioned below) is beneficial for the formation of interpenetrating nano-fibrillar networks.[36–38]

X-ray diffractions (XRD) of powdery polymer samples were also measured to investigate the packing of polymer chains in the solid state. As shown in Fig. S1,† **PCDPP** presents one peak in the wide angle region located at 23.71°, which corresponds to the π–π stacking distance between polymer backbones (d = 3.75 Å). Such a short π–π stacking distance indicates that **PCDPP** has a relatively planar conformation and can be closely stacked in the solid state.

BHJ polymer solar cells were fabricated with a conventional device structure of ITO/PEDOT : PSS/active layer/LiF/Al. A range of active layer compositions (weight ratios), spin-coating rates, and additives were systematically investigated. The active layer was deposited from chlorobenzene solutions without and with 1% 1,8-diiodooctane (DIO). The optimized donor (**PCDPP**) to acceptor ($PC_{71}BM$) weight ratio is 1 : 2 (w/w) and the optimized thickness is about 100 nm which was fabricated by spin-coating at a rate of 750 rpm with dilute blend solutions (polymer concentration: 3 mg mL^{-1}). Detailed information on device fabrication and measurements is given in the ESI.† The optimized device performance was achieved at a thickness of ~100 nm. The active layer was spin-coated at three different rates to adjust its thickness (see ESI†). When the active layer was fabricated at a low spin-coating rate of 500 rpm (thicker layer), a high short circuit current (J_{sc}) remained but the fill factor (FF) decreased, resulting in a slightly lower PCE relative to that with the optimal active layer thickness. The optimized **PCDPP**-based devices exhibited a maximum PCE of 9.02%, with an open circuit (V_{oc}) of 0.86 V, a short circuit current (J_{sc}) of 16.00 mA cm^{-2}, and a fill factor (FF) of 0.65. The detailed photovoltaic parameters are also summarized in Tables 1 and S1.† External quantum efficiency (EQE) measurements were performed to examine the response of devices to monochromatic light and the veracity of J_{sc} is obtained from J–V curves. As shown in Fig. 4, **PCDPP**-based devices exhibited a broad photo-to-current response in the range of 300 to 850 nm, corresponding to the UV-vis absorption spectrum. The highest EQE value of **PCDPP** approaches 70%, which is quite high for solar cells using DPP-based polymers.[11] We also summarize the device performance of DPP polymer solar cells in Table S2;† there are only three other examples with PCE over 8%. The calculated J_{sc} obtained from the EQE curve is 15.25 mA cm^{-2}, which is within 5% deviation from that obtained from the J–V curve. As mentioned above, due to the appropriate energy levels and optical bandgap, **PCDPP** shows a high V_{oc} and lower energy loss in devices. The planar geometry of **PCDPP** is conducive to molecular stacking and endows the blend film with higher mobility, which benefits the improvement of J_{sc}.

To characterize the charge transport ability of **PCDPP**, the hole mobility of BHJ solar cells was measured by using the space charge limited current (SCLC) model and calculated according to the equations reported in the literature. The details are shown in the ESI.† The hole mobility of the **PCDPP**-based device was calculated to be 1.8×10^{-4} cm^2 V^{-1} s^{-1}. The morphology of the **PCDPP** : $PC_{71}BM$ blend film was investigated by atomic

Table 1 Photovoltaic parameters of **PCDPP**-based devices with different additive ratios

CB (DIO)	V_{oc} (V)	J_{sc} (mA cm^{-2})	FF (%)	PCE $(\%)_{max}$
0.5%	0.87	14.1	0.68	8.25
1%	0.86	16.0	0.65	9.02
1.5%	0.87	15.6	0.63	8.55

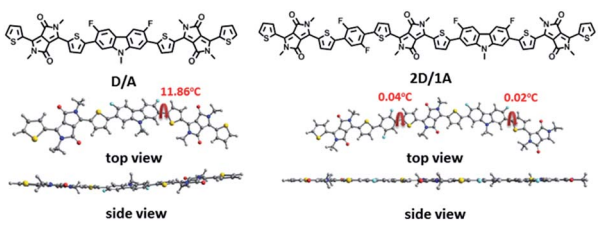

Fig. 3 Optimized geometries using DFT evaluated at the B3LYP/6-31G(d) level.

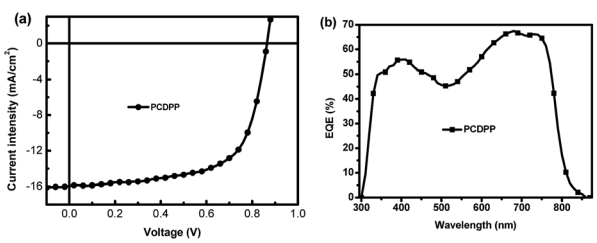

Fig. 4 J–V curve (a) and EQE curve (b) of **PCDPP** based devices.

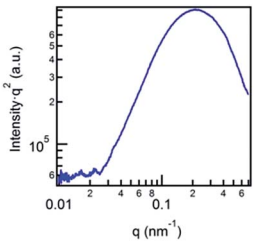

Fig. 5 R-SoXS of **PCDPP** based blend films.

force microscopy (AFM) in the tapping mode and transmission electron microscopy (TEM), and the details are shown in the ESI.† From the AFM measurements, the surface of this blend film is very smooth with a root-mean-square (RMS) of 1.48 nm. As shown in the TEM image of the blend film (Fig. S2†), **PCDPP** forms an extended fibrillar network in blends with $PC_{71}BM$ with a width of about 10 nm, which is beneficial for exciton diffusion and charge separation, affording a high J_{sc} and external quantum efficiencies.

Resonant soft X-ray scattering (R-SoXS) was also employed to probe the phase separation of the blends in the bulk under different conditions. A photon energy of 284.2 eV was selected to provide highly enhanced material contrast. Fig. 5 shows the R-SoXS profiles of the **PCDPP** : $PC_{71}BM$ blend film. The median of the distribution of the scattering s_{median} corresponds to the characteristic median length scale, ξ, of the corresponding log-normal distribution in real space with $\xi = 1/s_{median}$, which is a model independent statistical quantity. The **PCDPP** : $PC_{71}BM$ blend film shows a small ξ of ~30 nm which means the formation of appropriate phase separation at a small length scale in the blend film.[39] It is known that small domains are favorable for effective charge dissociation and thus the high J_{sc}.

Conclusions

In summary, a novel conjugated DPP-based polymer (**PCDPP**) with a medium bandgap was designed and synthesized *via* regular alternating ternary copolymerization. This polymer shows a broad absorption in the visible region and has low-lying HOMO and LUMO levels. The incorporation of 2,5-difluorobenzene as the second donor unit can improve the planarity of the polymer backbone with small dihedral angles approaching zero degrees from DFT calculations. Such a structure can facilitate the π–π stacking of polymer chains and forms a fibrillar network in blends with $PC_{71}BM$. After optimization of the device fabrication conditions, a maximum PCE of 9.02% has been achieved with a large V_{oc} of 0.86 V, a small energy loss of 0.69 eV, and a high J_{sc} of 16.00 mA cm^{-2}. We conclude that the high performance of **PCDPP**-based devices is due to the combinational results of the molecular structure with regular alternating 2D/1A units, the planar polymer backbone, and the appropriate optical bandgap and energy levels. Our results demonstrate that both a high J_{sc} and a large V_{oc} can be simultaneously achieved in high-efficiency solar cells using DPP-based polymers. This is achieved by using a polymer donor with a 2D/1A structure *via* regular alternating ternary copolymerization to reduce the energy loss in the active layer. Our results pave the way for realizing high-efficiency solar cells with large V_{oc} by using DPP-based polymers.

Experimental section

The original materials **1**, **2** and **5** were synthesized according to the previous literature.[2,31,32]

6,6′-(5,5′-(2,5-Difluoro-1,4-phenylene)bis(thiophene-5,2-diyl)) bis(2,5-bis(2-hexyldecyl)-3-(thiophen-2-yl)pyrrolo[3,4-*c*] pyrrole-1,4(2*H*,5*H*)-dione) (3)

A mixture of **1** (884 mg, 2.41 mmol), **2** (4 g, 4.82 mmol), $NaHCO_3$ (1.21 g, 14.28 mmol), H_2O (2 mL) and THF (40 mL) was carefully degassed several times and $Pd(PPh_3)_4$ (167 mg, 145 μmol) was added quickly. The reaction mixture was stirred at 90 °C under nitrogen for 24 hours. After cooling to room temperature, water was added and the mixture was extracted with DCM. The organic layer was dried with anhydrous $MgSO_4$, and evaporated to dryness. The residue was chromatographically purified on a silica gel column with DCM/petroleum ether (1 : 2, v/v) as the eluent to give **3** as a blue solid 3.14 g (81%). ^{1}H NMR (400 MHz, $CDCl_3$) δ: 8.88 (d, $J = 4$ Hz, 2H), 8.84 (d, $J = 4$ Hz, 2H), 7.60 (d, $J = 4$ Hz, 2H), 7.57 (d, $J = 4.9$ Hz, 2H), 7.47–7.43 (m, 2H), 7.22–7.19 (m, 2H), 4.01–3.96 (m, 8H), 1.87 (m, 4H), 1.27–1.15 (m, 96H), and 0.78–0.76 (m, 24H). ^{13}C NMR (100 MHz, $CDCl_3$) δ: 161.70, 161.64, 156.14, 154.17, 140.78, 140.03, 139.41, 135.89, 135.59, 130.93, 130.80, 129.80, 128.49, 127.94, 122.01, 121.92, 115.32, 115.07, 108.84, 108.12, 46.30, 38.05, 37.76, 31.89, 31.80, 31.78, 31.32, 31.19, 30.07, 30.03, 29.74, 29.69, 29.55, 29.52, 29.31, 26.33, 26.21, 26.18, 22.68, 22.65, 14.12, and 14.10.

6,6′-(5,5′-(2,5-Difluoro-1,4-phenylene)bis(thiophene-5,2-diyl)) bis(3-(5-bromothiophen-2-yl)-2,5-bis(2-hexyldecyl)pyrrolo[3,4-*c*]pyrrole-1,4(2*H*,5*H*)-dione) (4)

A solution of **3** (3.5 g, 2.17 mmol) in chloroform (50 mL) was protected from light and cooled to 0 °C. NBS (813 mg, 4.34 mmol) was added carefully into the mixture. And then, the solution was allowed to warm to room temperature and left to react for 12 hours. Chloroform was removed with a rotary evaporator. The residue was chromatographically purified on a silica gel column with DCM/petroleum ether (1 : 1, v/v) as an eluent to get **4**. The solid was recrystallized from a mixture of DCM and *n*-hexane to obtain pure product **4** as a blue solid 2.5 g (66%). ^{1}H NMR (400 MHz, $CDCl_3$) δ: 8.86 (d, $J = 4$ Hz, 2H), 8.57 (d, $J = 4$ Hz, 2H), 7.57 (d, $J = 4$ Hz, 2H), 7.43–7.39 (m, 2H), 7.13 (d, $J = 4$ Hz, 2H), 3.97 (d, $J = 11.6$ Hz, 4H), 3.87 (d, $J = 11.6$ Hz, 4H), 1.86–1.82 (m, 4H), 1.27–1.15 (m, 96H), and 0.78–0.76 (m, 24H). ^{13}C NMR (100 MHz, $CDCl_3$) δ: 161.29, 161.19, 156.01, 154.02, 140.20, 139.47, 139.14, 135.95, 135.47, 131.31, 131.19, 130.87, 127.86, 121.78, 121.68, 121.59, 119.09, 114.99, 114.74, 108.51, 108.10, 46.32, 37.95, 37.74, 31.90, 31.80, 31.33, 30.08, 29.75, 29.69, 29.55, 29.33, 26.33, 26.22, 26.19, 22.68, 22.65, and 14.12. Anal. calcd for $C_{98}H_{142}Br_2F_2N_4O_4S_4$: C 66.64, H 8.10, and N 3.17. Found: C 66.71, H 8.09, and N 3.14.

PCDPP

A mixture of monomer **4** (205.22 mg, 116.2 μmol), 9-(2-ethylhexyl)-3,6-difluoro-2,7-bis(4,4,5,5-tetramethyl-1,3,2-dioxaborolan-2-yl)-9*H*-carbazole (65.9 mg, 116.2 μmol), $NaHCO_3$ (1 g, 11.9 mmol), THF (20 mL), toluene (5 mL), and H_2O (2 mL) was added to a 100 mL Schlenk bottle and carefully degassed before and after $Pd(PPh_3)_4$ (4 mg, 3.5 μmol) was added. The mixture was stirred and refluxed at 100 °C for 72 h. Then, phenylboronic acid and $Pd(PPh_3)_4$ (4 mg) were added and refluxed for 4 h, and then bromobenzene was added and refluxed overnight to complete the end-capping reaction. After cooling to room temperature, the mixture was poured into 200 mL methanol. Then the solid was filtered and washed by Soxhlet extraction with water, methanol, acetone, hexane, and chloroform. The residue was dissolved in boiling TCE, filtered hot and precipitated in methanol to afford **PCDPP** as a dark green solid. Due to its low solubility in common solvents ($CHCl_3$, chlorobenzene, dichlorobenzene and so on), we can't get the ^1H NMR and ^{13}C NMR spectra of this polymer.

Acknowledgements

Financial support from the National Natural Science Foundation of China (91233205, 21161160443, 21534003 and 51273020), the Program for Changjiang Scholars and Innovative Research Team in University and the Fundamental Research Funds for the Central Universities is gratefully acknowledged.

Notes and references

1 R. S. Ashraf, I. Meager, M. Nikolka, M. Kirkus, M. Planells, B. C. Schroeder, S. Holliday, M. Hurhangee, C. B. Nielsen and H. Sirringhaus, *J. Am. Chem. Soc.*, 2015, **137**, 1314–1321.
2 K. H. Hendriks, G. H. L. Heintges, V. S. Gevaerts, M. M. Wienk and R. A. J. Janssen, *Angew. Chem., Int. Ed.*, 2013, **52**, 8499–8502.
3 W. Li, A. Furlan, W. S. Roelofs, K. H. Hendriks, G. W. van Pruissen, M. M. Wienk and R. A. Janssen, *Chem. Commun.*, 2013, **50**, 679–681.
4 W. Li, K. H. Hendriks, A. Furlan, W. S. C. Roelofs, M. M. Wienk and R. A. J. Janssen, *J. Am. Chem. Soc.*, 2013, **135**, 18942–18948.
5 W. Li, W. S. C. Roelofs, M. M. Wienk and R. A. J. Janssen, *J. Am. Chem. Soc.*, 2012, **134**, 13787–13795.
6 M. Grzybowski and D. T. Gryko, *Adv. Opt. Mater.*, 2015, **3**, 280–320.
7 J. Gao, L. Dou, W. Chen, C. C. Chen, X. Guo, J. You, B. Bob, W. H. Chang, J. Strzalka and C. Wang, *Adv. Energy Mater.*, 2014, **4**, 86–91.
8 W. Li, K. H. Hendriks, W. S. C. Roelofs, Y. Kim, M. M. Wienk and R. A. J. Janssen, *Adv. Mater.*, 2013, **25**, 3182–3186.
9 H. Choi, S. J. Ko, T. Kim, P. O. Morin, B. Walker, B. H. Lee, M. Leclerc, J. Y. Kim and A. J. Heeger, *Adv. Mater.*, 2015, **27**, 3318–3324.
10 K. H. Hendriks, W. Li, M. M. Wienk and R. A. Janssen, *J. Am. Chem. Soc.*, 2014, **136**, 12130–12136.
11 W. Li, K. H. Hendriks, M. M. Wienk and R. A. J. Janssen, *Acc. Chem. Res.*, 2016, **49**, 78–85.
12 A. P. Zoombelt, S. G. J. Mathijssen, M. G. R. Turbiez, M. M. Wienk and R. A. J. Janssen, *J. Mater. Chem.*, 2010, **20**, 2240–2246.
13 J. W. Jung, F. Liu, T. P. Russell and W. H. Jo, *Chem. Commun.*, 2013, **49**, 8495–8497.
14 C. Wang, *J. Mater. Chem. A*, 2016, **4**, 3477–3486.
15 D. Dang, X. Wang, Y. Zhi, L. Meng, X. Bao, R. Yang and W. Zhu, *Org. Electron.*, 2016, **32**, 237–243.
16 B. K. Sang, H. A. Um, H. J. Kim, J. C. Min and H. C. Dong, *Org. Electron.*, 2016, **31**, 198–206.
17 B. Jiang, C. C. Du, M. J. Li, K. Gao, L. Kou, M. Chen, F. Liu, T. P. Russell and H. Wang, *Polym. Chem.*, 2016, **7**, 3311–3324.
18 H. Yao, H. Zhang, L. Ye, W. Zhao, S. Zhang and J. Hou, *ACS Appl. Mater. Interfaces*, 2016, **8**, 3575–3583.
19 K. Kawashima, Y. Tamai, H. Ohkita, I. Osaka and K. Takimiya, *Nat. Commun.*, 2015, **6**, 10085, DOI: 10.1038/ncomms10085.
20 J. W. Lee, H. Ahn and W. H. Jo, *Macromolecules*, 2015, **48**, 7836–7842.
21 J. W. Jung, *Energy Environ. Sci.*, 2013, **6**, 3301–3307.
22 P. Shen, H. Bin, L. Xiao and Y. Li, *Macromolecules*, 2013, **46**, 9575–9586.
23 L. Wang, S. Shi, D. Ma, S. Chen, G. Chen, M. Wang, K. Shi, Y. Li, X. Li and H. Wang, *Macromolecules*, 2015, **48**, 287–296.
24 J. H. Kim, H. U. Kim, I. N. Kang, K. L. Sang, S. J. Moon, W. S. Shin and D. H. Hwang, *Macromolecules*, 2012, **45**, 8628–8638.
25 K. H. Kim, S. Park, H. Yu, H. Kang, I. Song, J. H. Oh and B. J. Kim, *Chem. Mater.*, 2014, **26**, 6963–6970.
26 C. Piliego, T. W. Holcombe, J. D. Douglas, C. H. Woo, P. M. Beaujuge and J. M. J. Fréchet, *J. Am. Chem. Soc.*, 2010, **132**, 7595–7597.
27 J. Rivnay, M. F. Toney, Y. Zheng, I. V. Kauvar, Z. Chen, V. Wagner, A. Facchetti and A. Salleo, *Adv. Mater.*, 2010, **22**, 4359–4363.
28 J. Mei, D. H. Kim, A. L. Ayzner, M. F. Toney and Z. Bao, *J. Am. Chem. Soc.*, 2011, **133**, 20130–20133.
29 K. H. Hendriks, G. H. L. Heintges, M. M. Wienk and R. A. J. Janssen, *J. Mater. Chem. A*, 2014, **2**, 17899–17905.
30 Q. Tao, Y. Xia, X. Xu, S. Hedström, O. Bäcke, D. I. James, P. Persson, E. Olsson, O. Inganäs, L. Hou, W. Zhu and E. Wang, *Macromolecules*, 2015, **48**, 1009–1016.
31 J. H. Park, E. H. Jung, J. W. Jung and W. H. Jo, *Adv. Mater.*, 2013, **25**, 2583–2588.
32 C. Du, W. Li, Y. Duan, C. Li, H. Dong, J. Zhu, W. Hu and Z. Bo, *Polym. Chem.*, 2013, **4**, 2773–2782.
33 Y. Liu, W. Zhao, Y. Wu, J. Zhang, G. Li, W. Li, W. Ma, J. Hou and Z. Bo, *J. Mater. Chem. A*, 2016, **4**, 8097–8104.
34 L. J. A. Koster, V. D. Mihailetchi and P. W. M. Blom, *Appl. Phys. Lett.*, 2006, **88**, 243502–243503.
35 C. J. Brabec, C. Winder, N. S. Sariciftci, J. C. Hummelen, A. Dhanabalan, H. P. A. Van and R. A. J. Janssen, *Adv. Funct. Mater.*, 2002, **12**, 709–712.

36 R. Qin, W. Li, C. Li, C. Du, C. Veit, H. F. Schleiermacher, M. Andersson, Z. Bo, Z. Liu and O. Inganäs, *J. Am. Chem. Soc.*, 2009, **131**, 14612–14613.
37 M. A. Uddin, T. H. Lee, S. Xu, Y. P. Song, T. Kim, S. Song, T. L. Nguyen, S. Ko, S. Hwang and Y. K. Jin, *Chem. Mater.*, 2015, **27**, 5997–6007.
38 T. L. Nguyen, H. Choi, S. J. Ko, M. A. Uddin, B. Walker, S. Yum, J. E. Jeong, M. H. Yun, T. J. Shin and S. Hwang, *Energy Environ. Sci.*, 2014, **7**, 3040–3051.
39 W. Ma, J. R. Tumbleston, M. Wang, E. Gann, F. Huang and H. Ade, *Adv. Energy Mater.*, 2013, **3**, 826.